Performance Analysis of DFIG based Wind Energy Conversion System Using Direct Power Controller

V. Kaarthikeyan[1], G. Madusudanan[2]

[1]Student, Valliammai Engineering College, Chennai, Tamil Nadu, India

[2]Assistant Professor, Valliammai Engineering College, Chennai, Tamil Nadu, India

Abstract: *In this paper, Direct Power Control (DPC) is introduced for the DFIG based wind energy conversion systems under distorted conditions. DFIG is very sensitive to grid disturbances and it experiences many problems such as distorted stator or rotor current, electromagnetic torque and power oscillations. The fifth and seventh order harmonics under distorted condition are analyzed in this paper. The harmonics level of those harmonics is reduced by using Vector Proportional Integrated Regulator. The steady state and stability consideration of the proposed regulator has been analyzed. With its fast dynamic response, the regulator has full voltage and power control; the smooth real and reactive power output can be achieved. The simulation is done by using MATLAB/SIMULINK software.*

Keywords: Direct power control, DFIG, Level of Harmonics, Vector Proportional Integrated regulator (VPI)

1. Introduction

Doubly fed induction generator (DFIG)-based wind turbine has become increasingly popular due to its advantage of variable speed operation with the excitation converter rated at only 25%−30% of the generator rating. However, since the stator of DFIG is directly connected to the grid and the power rating of its excitation converter is limited, the DFIG system is quite sensitive to grid disturbances. As the power penetration from the DFIG-based wind turbines into the grid is increasing steadily, the control and operation of DFIG under grid disturbances has become the subject of intense research during the last few years [1]–[10].

Of all grid disturbances, the unbalanced grid faults happen much more frequently than the balanced ones. The most severe problems of the DFIG under unbalanced faults are the oscillations of stator output power and electromagnetic torque, which are harmful to the stability of the connected power grid and the mechanical system of the wind turbine [1]. Moreover, voltage ripples will be produced in the dc-link as a result of power oscillations in the DFIG and the grid side converter (GSC), which is harmful to the dc-link capacitance.

To overcome the problem of harmonics several control techniques are introduced with different controllers such as hysteresis regulator [4], proportional- resonant regulator (PR) [2],[18]-[21], traditional PI regulator, proportional integral resonant (PIR) regulator, vector proportional integrated (VPI) regulator[2],[18].

Under harmonically distorted grid conditions, the DFIG contains six times the grid frequency pulsation item and average item of stator active and reactive power. Therefore, PI does not have the sufficient gain which is not appropriate. Similarly, PIR regulator would achieve zero steady- state error in which the PI and resonant part is used to deal with the average item and the pulsation item respectively. However, unexpected peak of magnitude response at the frequency larger than resonant 300 Hz may arise due to the

pole distribution of control object DFIG, which is detrimental to the stable closed-loop operation. Considering that it needs one specific resonant controller to deal with one specific harmonic sequence in the PR regulator, the control loop structure complexity would increase as the number of harmonic sequence increases, which is harmful to the stable closed-loop operation. The VPI regulator, based on pole-zero cancellation to avoid the unexpected gain peak [21], can be used to remove the DFIG stator active and reactive power pulsation components due to the adequate closed-loop phase margin and accurate AC signal tracking capability.

This paper proposes the direct power control strategy with vector proportional integrated regulator. By this technique, the harmonic level of the output stator voltages is reduced and the smooth real and reactive power can be achieved. The stator active and reactive power which has reduced oscillations or no oscillations is assumed as the control target of this strategy. Then, focused on the steady- state tracking accuracy, dynamic performance, stability as well as the rejection capability of the grid voltage distorted component and rejection capability of the grid voltage distorted component and back EMF compensation item, the performance analysis of the power control strategy with VPI regulator is conducted by using the mathematical and FFT analysis of the DFIG based wind energy conversion.

2. Mathematical modeling of DFIG

In order to perform the direct power control over DFIG, the mathematical analysis of DFIG is established. As we know both the Stator and rotor of the DFIG is fed by grid and converters, the required voltage to energize the stator and rotor is represented by separate voltage sources. The self and mutual inductances of the stator and rotor are considered in the equivalent model of the DFIG.

The equivalent T representation of DFIG is shown below.
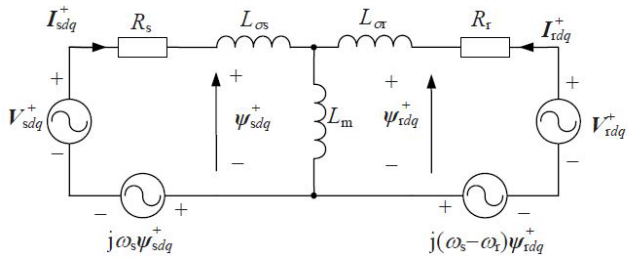
Figure 1: Equivalent T representation of DFIG

From the equivalent circuit of the DFIG, stator and rotor fluxes with respective d and q axis is represented as,

$$\Psi_{sdq} = L_s I_{sdq} + L_m I_{rdq} \quad (2.1)$$

$$\Psi_{rdq} = L_m I_{sdq} + L_r I_{rdq} \quad (2.2)$$

In the above equations the self inductances L_s and L_r is represented as

$$L_s = L_{\sigma s} + L_m \quad (2.3)$$

$$L_r = L_{\sigma r} + L_m \quad (2.4)$$

By solving the equations (2.1) and (2.2), we can determine I_{rdq} as follows,

$$I_{rdq} = \frac{L_m}{L_s L_r - L_m^2} \left(\frac{L_s}{L_m} \Psi_{rdq} - \Psi_{sdq} \right) \quad (2.5)$$

Similarly the current I_{sdq} can be determined as,

$$I_{sdq} = \frac{Lm}{LmLr - L_m^2} \left(\frac{L_r}{L_m} \Psi_{sdq} - \Psi_{rdq} \right) \quad (2.6)$$

From the equivalent circuit,

$$V_{sdq} = R_s I_{sdq} + \frac{d\Psi_{sdq}}{dt} + j\omega \Psi_{sdq} \quad (2.7)$$

$$V_{rdq} = R_r T_{rdq} + \frac{d\Psi_{rdq}}{dt} + j\omega \Psi_{rdq} \quad (2.8)$$

Output power can be expressed as,

$$P_s + jQ_s = \frac{3}{2} V_{sdq} I_{sdq} \quad (2.9)$$

Equation (2.7) can be written as,

$$V_{sdq} = V_{sd} = -\omega_s \Psi_{sq} \quad (2.10)$$

Substituting eqn (2.5) and (2.10) in eqn (2.9)

$$P_s + jQ_s = -k_\sigma V_{sd} \Psi_{rd} + jk_\sigma V_{sd} \left(\frac{L_r}{L_m} \frac{V_{sd}}{\omega} + \Psi_{rq} \right) \quad (2.11)$$

Where

$$k_\sigma = \frac{3}{2} \left(\frac{L_m}{L_r L_s - L_m^2} \right) \quad (2.12)$$

From equation (2.11)

$$P_s = -k_\sigma V_{sd} \Psi_{rd} \quad (2.13)$$

$$Q_s = k_\sigma V_{sd} \left(\frac{L_r}{L_m} \frac{V_{sd}}{\omega} + \Psi_{rq} \right) \quad (2.14)$$

From eqn (2.13)

$$\Psi_{rd} = \frac{P_s}{k_\sigma V_{sd}} \quad (2.15)$$

From eqn (2.14) we can determine,

$$\Psi_{rq} = \frac{Q_s}{k_\sigma V_{sd}} - \frac{L_r}{L_m} \frac{V_{sd}}{\omega} \quad (2.16)$$

Separating the d and q components from the eqn (2.8)

$$V_{rd} = R_r I_{rd} + \frac{d\Psi_{rd}}{dt} - \omega \Psi_{rq} \quad (2.17)$$

$$V_{rq} = R_r I_{rq} + \frac{d\Psi_{rq}}{dt} + \omega \Psi_{rd} \quad (2.18)$$

By substituting 'd' component of the (2.6) and (2.15) into (2.17)

$$V_{rd} = -R_r \frac{L_s}{L_r L_s - L_m^2} \left(\frac{P_s}{k_\sigma V_{sd}} \right) - \frac{1}{k_\sigma V_{sd}} \left(\frac{dP_s}{dt} \right) - \omega \Psi_{rq} \quad (2.19)$$

The last term represented in the above equation is rotor back emf and it's effect is going to be compensated by the regulator.
Transfer function of real power to the rotor 'd' component voltage can be determined by taking laplace transform of the respective equarions. After taking laplace transform of the equations, we get the transfer function as,

$$\frac{P_s(s)}{V_{rd}(s)} = \frac{3}{2} \frac{V_{sd} L_m}{L_s (R_r + s\sigma L_r)} \quad (2.20)$$

Here

$$\sigma = \frac{L_s L_r - L_m^2}{L_s L_r}$$

Similarly the transfer function between the ractive power and rotor voltage 'q' component is determined as,

$$\frac{Q_s(s)}{V_{rq}(s)} = \frac{3}{2} \frac{L_m V_{sd}}{L_s (R_r + s\sigma L_r)} \quad (2.21)$$

By using equations (2.15) and (2.16) during a sampling period Ts, we can write

$$\frac{d\Psi_{rd}}{dt} = \frac{-1}{k_\sigma V_{sd}} \frac{P_s^* - P_s}{T_s} \quad (2.22)$$

$$\frac{d\Psi_{rq}}{dt} = \frac{1}{k_\sigma V_{sd}} \frac{Q_s^* - Q_s}{T_s} \quad (2.23)$$

By substituting eqns (2.22) &(2.23) and (2.15)&(2.16) in eqn (2.17) we can get,

$$V_{rd} = -C_{VPI}(s)(P_s^* - P_s) - \omega_s \left(\frac{Q_s}{k_\sigma V_{sd}} - \frac{L_r}{L_m} \frac{V_{sd}}{\omega} \right) \quad (2.24)$$

$$V_{rq} = C_{VPI}(s)(Q_s^* - Q_s) - \omega_s \left(\frac{P_s}{k_\sigma V_{sd}} \right) \quad (2.25)$$

Here Cvpi represents the coefficient of vector proportional integrated controller.

3. Performance Analysis of power control scheme with VPI regulator

To achieve the smooth stator active and reactive power during the grid disturbances, the VPI regulator is

Paper ID: SUB15497
1348

implemented in the power control scheme. Thus the harmonics level can be reduced and the smooth real and reactive power can be achieved.

Transfer function of Vector Proportional Integrated regulator is as follows [2],[18]

$$C_{VPI} = K_p + \frac{K_i}{s} + \frac{K_{pr} + s^2 + K_{ir}s}{s^2 + \omega_c s + \omega_0^2} \quad (3.1)$$

In the transfer function of VPI, Kp and Ki are the proportional and integral coefficients. Similarly the Kpr, Ki are the proportional and integral of the VPI regulator to regulate the harmonic components. Kir is calculated based on pole-zero cancellation.

It can be calculated as,

$$K_{ir} = \frac{K_{pr} R_r}{\sigma L_r} \quad (3.2)$$

In the direct power control scheme of DFIG is only the regulator parameters are adjusted in the control loop. Resonant frequency (ω_0) and Machine parameters are fixed.

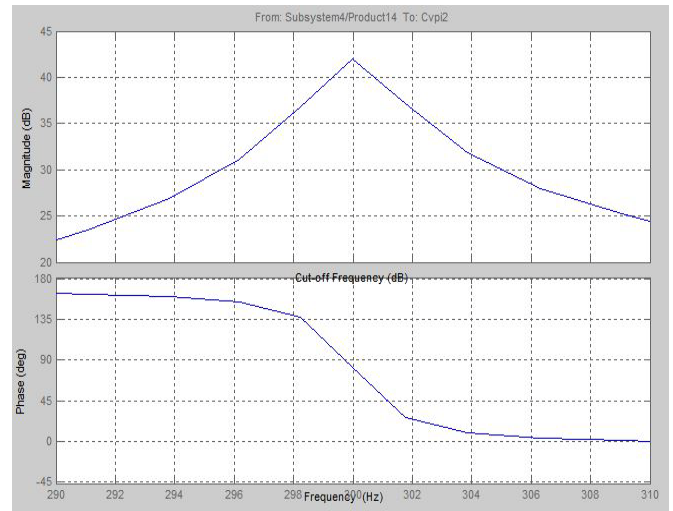### 3.1 Frequency response of VPI regulator

Frequency response for the VPI regulator is performed to determine the gain of the regulator at different cut off frequencies. By using the transfer function, for different values of proportional and integral coefficients the frequency analysis is done. The frequency response of the VPI can be analyzed with the help of the bode diagram. The bode diagram shown in figure 2, gives the frequency response of the regulator at cut off frequency ω_c=15 rad/s.

Table 1: VPI parameters

Parameters	Values
Kpr	1
Kir	157
Kp,Ki	1
ω_c	15 rad/s

Frequency response of the VPI regulator carried out with different gain values. From the bode diagram which shown here explain that the gain of regulator is maximum at the frequency 300Hz, at which the distorted grid operates with six times the grid frequency.

The magnitude at the resonant frequency 300 Hz is 42 dB, which is sufficient to minimize the control error.

Figure 2: Bode diagram of VPI with ω_c=15 rad/s, Kpr=1.0
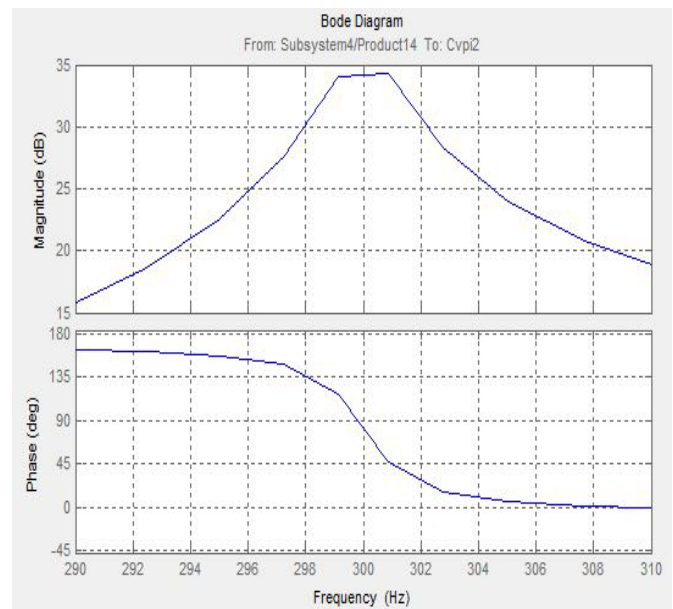
Figure 3: Bode diagram of VPI with ω_c=15 rad/s, Kpr=0.5

In Figure 3 frequency response of VPI with Kpr=0.5 is shown. The proportional gain of the regulator is reduced. From the previous mentioned bode diagrams,

Table 2: Frequency response for different Kpr values

Kpr with ω_c=15 rad/s	Magntitude (dB)
1	42
0.75	39.2
0.5	36.5

From the above mentioned table, it is clear that the magnitude is decreasing with decreased values of proportional coefficient (Kpr) of VPI regulator.

Paper ID: SUB15497

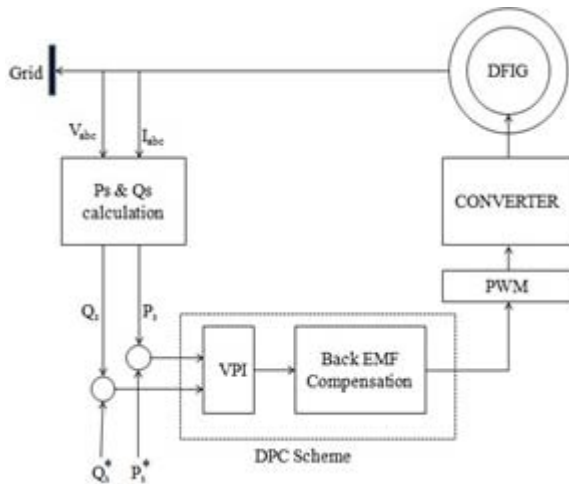## 4. Proposed Power control strategy with VPI

Figure 4: Direct power control of DFIG with VPI regulator

The block diagram shown in figure 4 explains the proposed direct power control strategy of DFIG with VPI regulator. With the help of equations derived in the section 2, the real and reactive power is calculated. The calculated power is compared with the reference real and reactive power. The direct power control scheme is implemented with VPI and back EMF compensation. The pulses required for the rotor side converter is being generated with the help of the regulators. The block diagram shown in the fig is simulated using the MATLAB/SIMULINK.
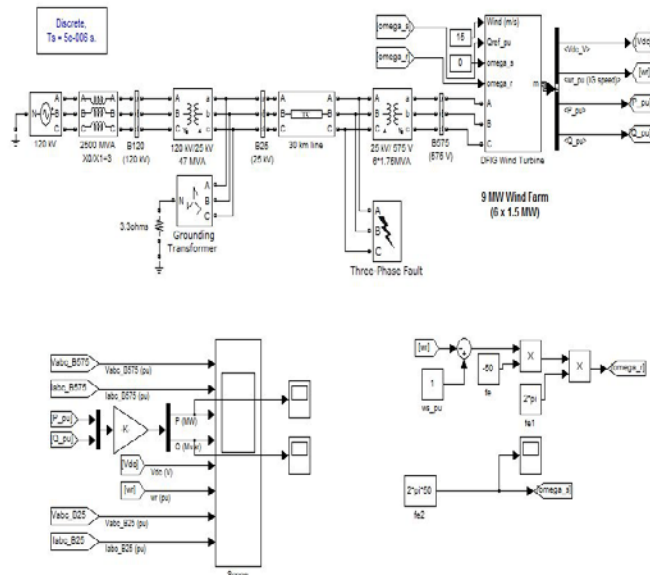
4.1 Simulation of the Proposed System

Figure 5: Simulation of the proposed system

In the simulation, 9MW wind farm which consists if six 1.5 MW wind turbines is used. This wind farm is connected to the 120 kV grid through 30 km transmission line through the transformer having ratings of 120 kV/25 kV on grid side as well as wind turbine side. To introduce a distorted condition in the grid, a single line to ground fault is considered in the transmission line.

4.2 Simulation results of the proposed system

The simulation mentioned in the fig is executed and from the wind turbine DC link voltage, Induction generator speed, real and reactive power is measured. The simulation is performed with two conditions i.e., with VPI enabled, with VPI disabled. Under fault conditions, i.e. distorted conditions, the simulated system is executed with VPI disabled. With this condition, the output voltage, real and reactive power is measured. The output results with disabled VPI is shown below.
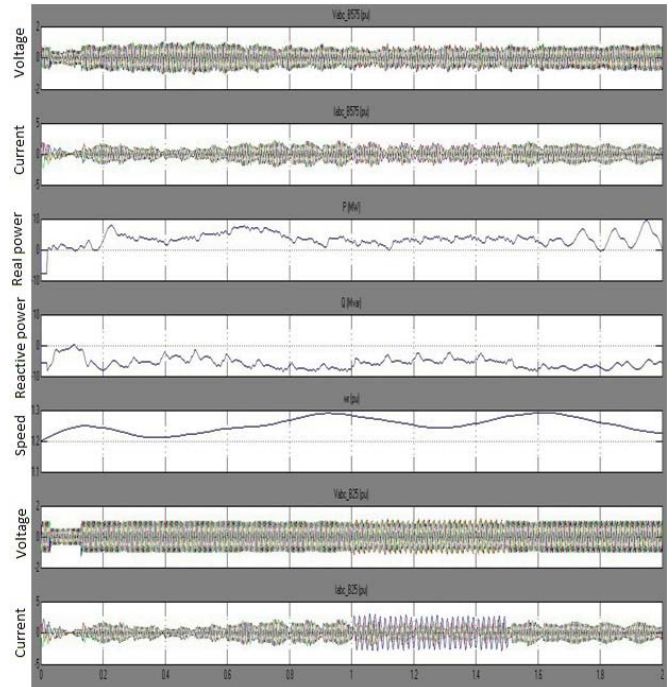

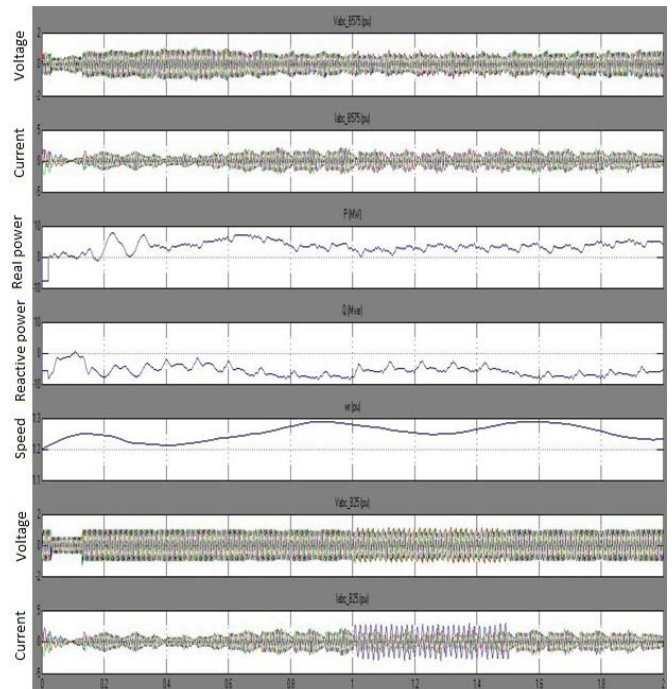**Figure 6:** Output waveforms with VPI disabled

Figure 7: Output waveforms with VPI enabled

Paper ID: SUB15497
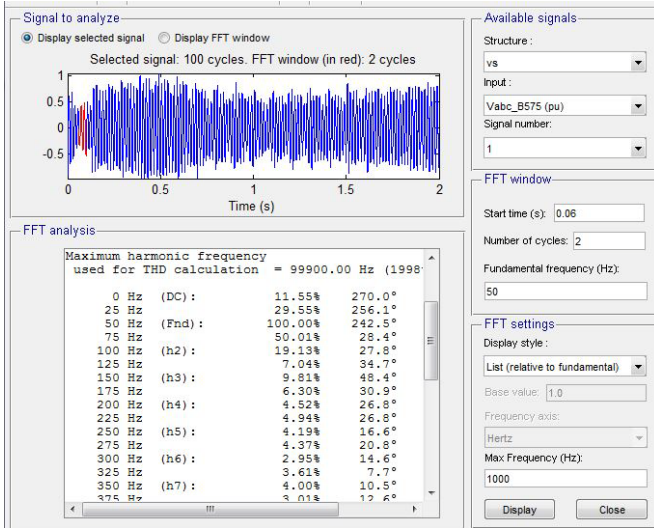
4.3 FFT Analysis

To determine the harmonics level in the output voltages, FFT analysis is performed. FFT analysis is done for both cases, with VPI enabled and with VPI enabled, at the base of fundamental frequency 50 Hz. From the FFT analysis, the list of harmonics in the output voltages is presented with percentage level of harmonics.
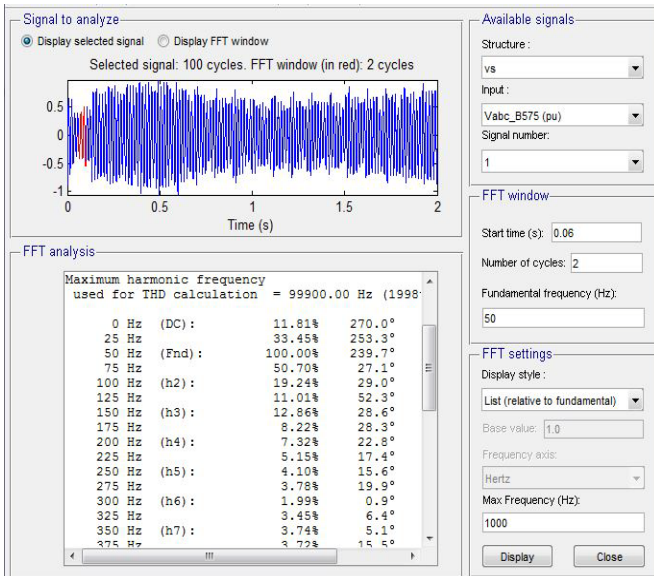

Figure 8: FFT analysis of the output voltage with VPI disabled

Figure 9: FFT analysis of the output voltage with VPI enabled

From the FFT analysis, we can compare the harmonic levels present in the output voltage at distorted condition. The amount of fifth and seventh order harmonics present during distorted conditions is high, with the VPI regulator is disabled. The VPI regulator is then enabled in order to reduce the harmonics level in the output voltage. As a result the harmonics level in the output voltage is reduced with the help of the VPI regulator.

Parameters of the wind turbine and the DFIG, the fault specifications are listed in the table below.

Table 3: Machine Parameters

Parameters	Values
Rr	0.016 p.u
Lr	0.16 p.u
Lm	2.9 p.u
P_{nom}	1.6 MW
V_{nom}	575 kV
F	50Hz
Pole pair (p)	3

Table 4: Fault details

Parameters	Values
Fault Resistance	1Ω
Ground Resistance	0.001Ω
Transition times	1/50 s,5/50 s
Type of fault	Phase a to ground fault (L-G type)

5. Conclusion

In this paper, Vector Proportional Integrated (VPI) controller is used in direct power control of the DFIG connected wind energy system. With help of VPI regulator, the level of the harmonics which produced due to the fault in the system is reduced. The percentage level of harmonic present in the system with VPI regulator and without VPI regulator is analyzed using FFT analysis and the results are compared. The frequency response of the vector proportional integrated controller under various conditions is discussed in this project. Simulated results of the distorted system with and without VPI also discussed. Also with help of VPI regulator, smooth real and reactive power is achieved. The efficiency of this technique can be improved by combining different type of the regulators, instead of using single regulator.

References

[1] Hu.J,He.Y, Xu.L, and Williams.B.W.(2009), "Improved control of DFIG systems during network unbalance using PI–R current regulators," *IEEE Trans. Ind. Electron.*, Vol. 56, No. 2, pp. 439–451.

[2] Lascu.C, Asiminoaei.L, Boldea.I, and Blaabjerg.F (2007), "High performance current controller for selective harmonic compensation in active power filters," *IEEE Trans. Power Electron.*, Vol. 22, No. 5, pp. 1826–1835.

[3] Liu.C, Blaabjerg.F, Chen.W, and Xu.D (2012), "Stator current harmonic control with resonant controller for doubly fed induction generator," *IEEE Trans. Power Electron.*, Vol. 27, No. 7, pp. 3207–3220.

[4] Mohseni.M, Islam.S.M, and Masoum.M.A (2011), "Enhanced hysteresisbased current regulators in vector control of DFIG wind turbines," *IEEE Trans. Power Electron.*, Vol. 26, No. 1, pp. 223–234.

[5] Nian.H, Song.Y, Zhou.P, and He.Y (2011), "Improved direct power control of a wind turbine driven doubly fed induction generator during transient grid voltage unbalance," *IEEE Trans. Energy Convers.*, Vol. 26, No. 3 pp. 976–986.

[6] Xu.L and Cartwright.P (2006), "Direct active and reactive power control of DFIG for wind energy

generation," *IEEE Trans. Energy Convers.*, Vol. 21, No. 3, pp. 750–758.

[7] Xu.L, Zhi.D, and Williams.B.W (2009), "Predictive current control of doubly fed induction generators," *IEEE Trans. Ind. Electron.*, Vol. 56, No. 10, pp. 4143–4153.

[8] Zhi.D and Xu.L (2007), "Direct power control of DFIG with constant switching frequency and improved transient performance," *IEEE Trans. Energy Convers.*, Vol. 22, No. 1, pp. 110–118.

[9] Zhi.D, Xu.L, and Williams.B.W (2010), "Model-based predictive direct power control of doubly fed induction generators," *IEEE Trans. Power Electron.*, Vol. 25, No. 2, pp. 341–351.

[10] Zhou.P, He.Y, and Sun.D (2009), "Improved direct power control of a DFIGbased wind turbine during network unbalance," IEEE Trans. Power Electron., Vol. 24, No. 11, pp. 2465–2474.

[11] Zmood.D.N and Holmes.D.G (2003), "Stationary frame current regulation of PWMinverterswith zero steady-state error," *IEEE Trans. Power Electron.*, Vol. 18, No. 3, pp. 814–822.

[12] R. Datta and V. T. Ranganathan, "Direct power control of grid-connected wound rotor induction machine without rotor position sensors," *IEEE Trans. Power Electron.*, vol. 16, no. 3, pp. 390–399, May 2001.

[13] V. Phan and H. Lee, "Control strategy for harmonic elimination in standalone DFIG applications with nonlinear loads," *IEEE Trans. Power Electron.*, vol. 26, no. 9, pp. 2662–2675, Sep. 2011.

[14] G. K. Singh, "Power system harmonics research: A survey," *Euro. TransElectr. Power*, vol. 19, no. 2, pp. 151–172, Aug. 2007.

[15] S. Muller, M. Deicke, and R. W. De Doncker, "Doubly fed induction generator systems for wind turbines," *IEEE Ind. Appl. Mag.*, vol. 8, no. 3, pp. 26–33, May/Jun. 2002.

[16] A. Luna, F. K. Lima, D. Santos, and P. Rodriguez, "Simplified modeling of a DFIG for transient studies in wind power applications," *IEEE Trans. Ind. Electron.*, vol. 58, no. 1, pp. 9–20, Jan. 2011

[17] L. Xu, "Coordinated control of DFIG's rotor and grid side converters during network unbalance," *IEEE Trans. Power Electron.*, vol. 23, no. 3, pp. 1041–1049, May 2008.

[18] C. Lascu, L. Asiminoaei, I. Boldea, and F. Blaabjerg, "Frequency response analysis of current controllers for selective harmonic compensation in active power filters," *IEEE Trans. Ind. Electron.*, vol. 56, no. 2, pp. 337– 347, Feb. 2009.

[19] D. N. Zmood, D. G. Holmes, and G. H. Bode, "Frequency-domain analysisof three-phase linear current regulators," *IEEE Trans. Ind. Appl.*, vol. 37, no. 2, pp. 601–610, Mar./Apr. 2001.

[20] D. N. Zmood and D. G. Holmes, "Stationary frame current regulation ofPWMinverterswith zero steady-state error," *IEEE Trans. Power Electron.*, vol. 18, no. 3, pp. 814–822, May 2003.

[21] G. Shen, X. Zhu, J. Zhang, and D. Xu, "A new feedback method for PR current control of LCL-filter-based grid-connected inverter," *IEEE Trans. Ind. Electron.*, vol. 57, no. 6, pp. 2033–2041, Jun. 2010.

Author Profile

V. Kaarthikeyan received the Bachelor's degree in Electrical and Electronics Engineering from St. Joseph's college of Engineering, Chennai in 2013 and he is pursuing Master's degree in Power Systems Engineering in Valliammai Engineering College, Chennai. His area of interest is power system and renewable energy scheme in power system.

G. Madusudanan received the Bachelor's degree in Electrical and Electronics Engineering from Bharathidasan University in 1997. He received his Master's degree in Power Electronics and Drives from Bharathidasan University in 2000. Now he is working as Assistant Professor in Valliammai Engineering College, Chennai.